*International Journal of Astrobiology* 16 (3): 286–292 (2017) doi:10.1017/S1473550416000367


# Raman spectroscopy of shocked gypsum from a meteorite impact crater

Connor Brolly, John Parnell and Stephen Bowden

*Department of Geology & Petroleum Geology, University of Aberdeen, Meston Building, Aberdeen, UK e-mail: c.brolly@abdn.ac.uk*

**Abstract**: Impact craters and associated hydrothermal systems are regarded as sites within which life could originate on Earth, and on Mars. The Haughton impact crater, one of the most well preserved craters on Earth, is abundant in Ca-sulphates. Selenite, a transparent form of gypsum, has been colonized by viable cyanobacteria. Basement rocks, which have been shocked, are more abundant in endolithic organisms, when compared with un-shocked basement. We infer that selenitic and shocked gypsum are more suitable for microbial colonization and have enhanced habitability. This is analogous to many Martian craters, such as Gale Crater, which has sulphate deposits in a central layered mound, thought to be formed by post-impact hydrothermal springs. In preparation for the 2020 ExoMars mission, experiments were conducted to determine whether Raman spectroscopy can distinguish between gypsum with different degrees of habitability. Ca-sulphates were analysed using Raman spectroscopy and results show no significant statistical difference between gypsum that has experienced shock by meteorite impact and gypsum, which has been dissolved and re-precipitated as an evaporitic crust. Raman spectroscopy is able to distinguish between selenite and unaltered gypsum. This shows that Raman spectroscopy can identify more habitable forms of gypsum, and demonstrates the current capabilities of Raman spectroscopy for the interpretation of gypsum habitability.

*Received 31 May 2016, accepted 19 August 2016, first published online 21 September 2016*

**Key words:** habitability, impact crater, Raman spectroscopy, shocked gypsum.

## Introduction

### *Impact generated sulphate deposits and significance for life*

Hydrothermal deposits within craters on Mars represent one of the most important targets in the search for life on Mars (Cabrol *et al.* 1999; Newsom *et al.* 2001). Hydrothermal systems are realistic sites to sustain life due to the presence of liquid $H_2O$, heat and dissolved nutrients and alkaline vents within these systems are considered to be locations where life could originate (Farmer & Des Marais 1999; Newsom *et al.* 2001; Osinski *et al.* 2005; Lane & Martin 2012). Over 60 impact craters with associated hydrothermal activity have been discovered on Earth, and given the long bombardment history of Mars, impact craters could be a common site to search for life (Chapman & Jones 1977; Naumov 2002). Gale Crater has sulphates present within a layered sedimentary mound in the centre of the crater, named Mount Sharp, thought to be formed by hydrothermal springs, as there is a lack of features associated with lacustrine environments such as terraces, deltas and fans. (Rossi *et al.* 2008; Thomson *et al.* 2011; Schwenzer *et al.* 2012). Semi-hydrated Ca-sulphate, bassanite has been identified in Mawrth Vallis, one of the proposed landing sites for the ExoMars 2020 mission (Wray *et al.* 2010).

The Eocene Haughton impact crater, located on Devon Island in the Canadian High Arctic Archipelago, provides a useful analogue site to study post impact sulphate deposits (Sherlock *et al.* 2005). It is exceptionally well preserved, which is why it has been extensively studied, and has examples of sulphate deposits containing microbial life (Osinski & Spray 2001; Parnell *et al.* 2004). The current structure is composed of a central uplift overlaid with melt breccia, which is the most common impactite (Lindgren *et al.* 2009). There is a gneissic crystalline basement, which is shocked and is inhabited by endolithic photosynthetic microorganisms. These organisms are more abundant in the shocked material due to an increased pore space as a result of impact fracturing, and increased translucence due to vaporization of opaque mineral phases (Cockell *et al.* 2002). The target rock included gypsum bearing carbonate rocks, Ordovician in age (Robertson & Sweeney 1983). Impact remobilized sulphate occurs as selenite, a transparent form of gypsum (CaSO4.2(H2O)), which cross-cuts the melt breccia as veins. Viable, extant cyanobacterial colonies are present within the selenite and are black in colour due to the UV protective pigments scytonemin and gloeocapsin (Cockell *et al.* 2002, 2003). Mobilization still occurs at present in the form of evaporitic crusts on bedrock surfaces and soil (Parnell *et al.* 2004).

Given that sulphates formed by hydrothermal activity are habitable substrates, and that shocking increases the space for an organism to exploit; shocked sulphates are important targets with which to find evidence of microbial life. If instrumentation could distinguish between shocked and un-shocked phases, and between various sulphate phases, this would be beneficial when identifying the most likely sulphates to contain life signatures.

### *Raman for Mars*

Raman spectroscopy uses a monochromatic laser light source to irradiate a sample. Majority of the light, which interacts

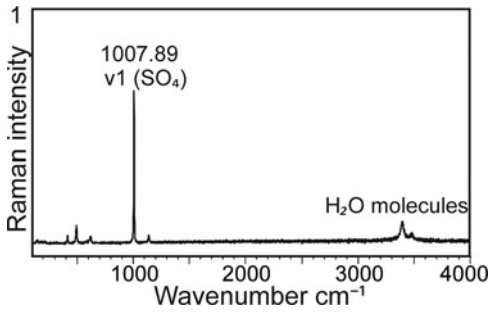


**Fig. 1.** Extended spectra 100–4000 $cm^{-1}$ showing v1 sulphate symmetric stretching mode (1007.89 $cm^{-1}$) and stretching mode of $H_2O$ ($\sim$3450 $cm^{-1}$).

with the sample is scattered elastically, with no change in wavelength. However a small proportion of the light is scattered inelastically – either an increase or decrease in wavelength, known as Raman scattering. Raman spectroscopy produces a vibrational 'fingerprint', which is dependent on the vibrational state of molecules in a given compound (Ellery & Wynn-Williams 2003).

The popularity of Raman spectroscopy has dramatically increased in the last 30 years due to its increasing range of applications (Pérez & Martinez-Frias 2006). It is a useful astrobiological tool as it is a non-destructive technique, which is able to be miniaturized. It is sensitive to carbonaceous materials, which is one of the main targets of the ESA ExoMars mission but it is also sensitive to various microbial pigments, such as chlorophylls, carotenoids and scytonemin, which increase its appeal (Ellery & Wynn-Williams 2003; Jehlička *et al.* 2014). It has a wavelength range covering most vibrational modes including carbonates, silicates and sulphates (i.e. most rock-forming minerals), therefore it can also be used for petrographic analysis (Haskin *et al.* 1997; Wang *et al.* 1998).

### *Raman spectroscopy of gypsum and impact shocked gypsum*

The Raman spectrum of gypsum characteristically shows a narrow intense band around 1008 reciprocal centimetres ($cm^{-1}$), which is the v1 sulphate symmetric stretching mode, herein referred to as v1 sulphate band. The stretching modes of water occur around 3450 $cm^{-1}$ (Berenblut *et al.* 1970; Krishnamurthy & Soots 1971), shown in Fig. 1.

The astrobiological community is interested in the effect of shocking on sulphates as they occur on Mars. Micro-scale deformation experiments of gypsum by Hogan *et al.* (2012), show that the v1 sulphate band is least intense at the centre of deformation, where most load was experienced, and most intense at the outer margins of the deformation structure where least load was experienced. This is evidence that shocking reduces the v1 sulphate stretching band intensity. Instantaneous compressional deformation occurs in both meteorite (macro) shock events and micro-indentation experiments.

The effects of shock on gypsum have been discussed by Ramkissoon *et al.* (2014), using impact shock experiments with a two stage light gas gun and projectile, fired at plaster of Paris (gypsum). Their experiments show that

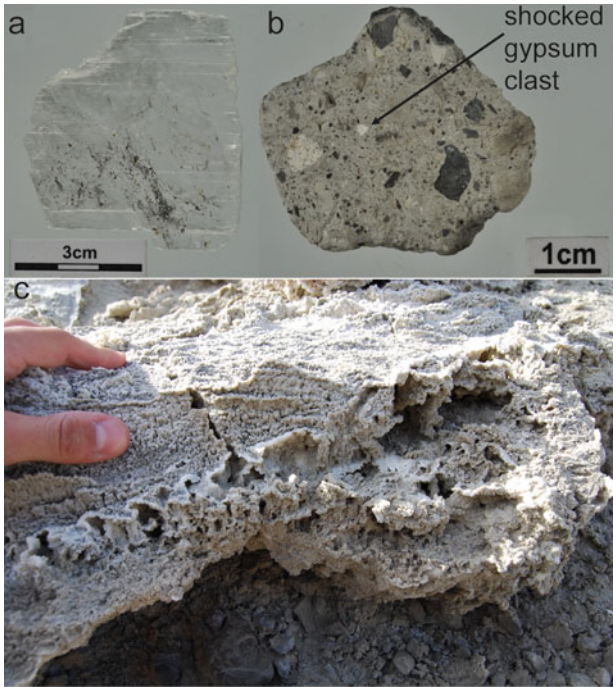


**Fig. 2.** Sample photographs. (a) Selenite, Haughton crater (S2), showing black pigmentation of bacterial colonies. (b) Melt breccia, Haughton crater (SH1), showing fragment of shocked gypsum. (c) Evaporitic gypsum crust, Haughton crater (C1).

Table 1. *Table of sample locations and ages*

| Sample | Description/location | Age | Group |
|---|---|---|---|
| U1 | Vale of Eden, Cumbria, UK | Permian | 1 |
| U2 | Kingscourt fibrous, Co. Cavan, Ireland | Triassic | 1 |
| U3 | Scapa, Orkney | Devonian | 1 |
| U4 | Kingscourt with hematite, Co. Cavan, Ireland | Triassic | 1 |
| U5 | Gotham Triassic, England | Triassic | 1 |
| U6 | Ebro Basin, Spain | Oligocene-Miocene | 1 |
| S1 | Selenite, California | Paleogene | 2 |
| S2 | Selenite, Haughton, Devon Island | Eocene-Oligocene | 2 |
| S3 | GSC dome (NE side), Selenite Haughton, Devon Island | Eocene-Oligocene | 2 |
| S4 | Selenite, Kent | Eocene | 2 |
| C1 | Central uplift crust, Haughton, Devon Island | Eocene-Holocene | 3 |
| C2 | GSC dome (NE side) crust, Haughton, Devon Island | Eocene-Holocene | 3 |
| C3 | Gypcrete Chile | Paleogene – Holocene | 3 |
| C4 | Rhino Creek, Crust on lake sediments, Haughton, Devon Island | Eocene-Holocene | 3 |
| SH1 | West Rhino creek melt breccia, Haughton, Devon Island | Eocene | 4 |
| SH2 | Gemini Hills Shocked A Haughton, Devon Island | Eocene | 4 |
| SH3 | Gemini Hills Shocked B Haughton, Devon Island | Eocene | 4 |

https://doi.org/10.1017/S1473550416000367 Published online by Cambridge University Press

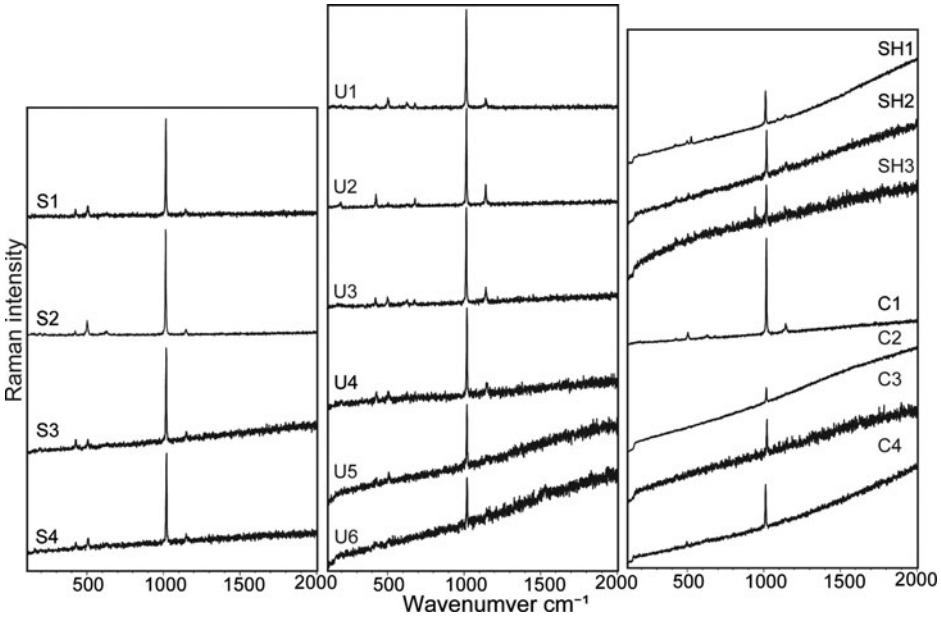


**Fig. 3.** Extended Raman spectra for gypsum (100–2000 $cm^{-1}$). *x*-axis is Raman shift in reciprocal centimetres ($cm^{-1}$). *y*-axis is Raman intensity in arbitrary units (a.u.). 'SH' spectra have experienced shock from meteoric impact. 'C' spectra are gypsum samples, which have been dissolved then re-precipitated as evaporitic crusts. 'S' spectra are selenite, a transparent form of gypsum. 'U' spectra are from unaltered gypsum samples unaffected by shock or dissolution and re-precipitation.

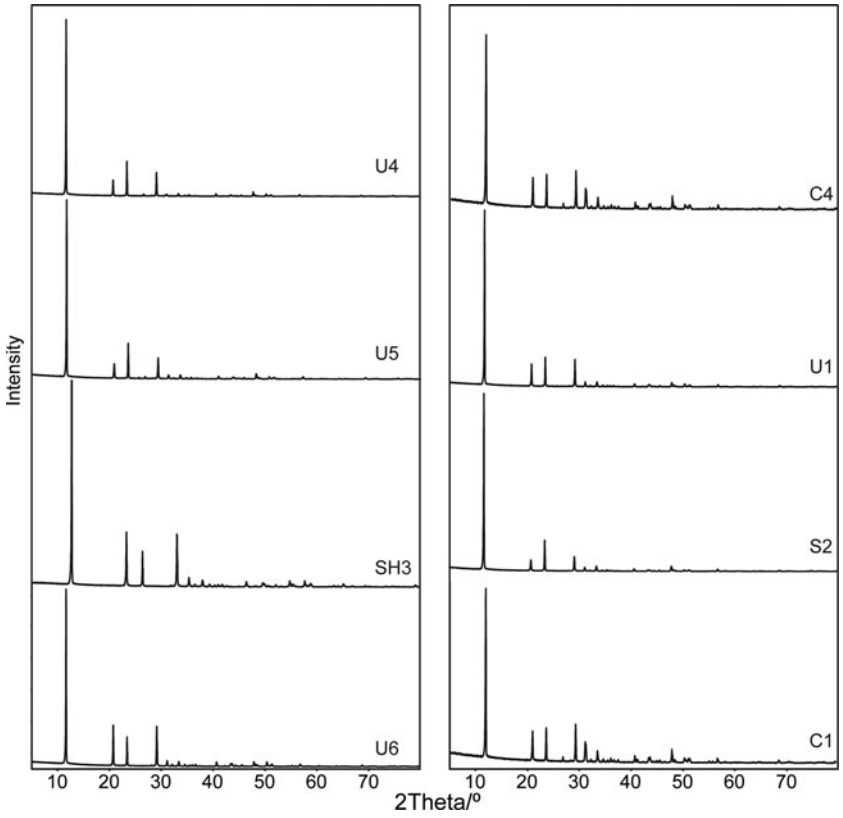


**Fig. 4.** X-ray diffraction patterns.

devolatilization occurs as a result of the impact, based on the disappearance of water molecule bands around 3450 $cm^{-1}$, and the shift of bands 427 and 487 $cm^{-1}$, is indicative of anhydrite. Characterizing the dehydration of gypsum to anhydrite using Raman spectroscopy has been well studied and shows the sulphate stretching band exhibiting an increase in band position with increasing dehydration (Prasad *et al.* 2001; Liu *et al.* 2009).

https://doi.org/10.1017/S1473550416000367 Published online by Cambridge University Press

Bucio *et al.* (2015) used experimentally impact-shocked gypsum to characterize post-impact phases using Raman spectroscopy and X-ray diffraction (XRD). This study compared Raman spectra obtained from naturally shocked samples with Raman spectra obtained from experimentally impact-shocked gypsum, published by previous authors, to assess if the spectral changes associated with shock are comparable, and ultimately if shocked gypsum can be differentiated from other phases of gypsum. The spectral changes were analysed by comparing v1 sulphate band positions against band widths, referred to as the full width at half maximum (FWHM).

## Methods

### *Samples*

Gypsum samples were separated into four groups:

(1) Unaltered gypsum – samples which have not experienced shock or dissolution and subsequent re-precipitation. The crystal habits range from grainy to massive or fibrous.
(2) Selenite – a transparent form of gypsum, which has a distinct platy crystal habit. Selenite at the Haughton structure formed by the dissolution of gypsum in the target rock, and circulated the structure before re-precipitating as selenite.
(3) Crusts – sulphate rich waters at the Haughton flows over the surface topography and slowly evaporates, leaving a mineral 'crust' on outcropped rock and soil.
(4) Shocked gypsum – samples include a primary shocked gypsum nodule, and shocked gypsum fragments within melt breccia (see Fig. 2).

The majority of the samples originate from the Haughton impact crater, Devon Island, Canada; see Table 1 for more information on sample locations and ages. Minimal sample preparation was employed, simulating capabilities during a remote mission on Mars. If necessary, samples were cut to expose the sulphate, however where possible rough untreated surfaces were analysed. This study would be equally appropriate for the NASA 2020, SHERLOC instrument, which will have spatial mapping capabilities (Beegle *et al.* 2015).

### *Raman spectroscopy configuration*

Raman spectra were obtained using a Renishaw InVia H36031 confocal Raman microscope operating at a wavelength of 514.5 nm green monochromatic laser light, which is similar to the ExoMars flight instrument wavelength of 532 nm (Rull *et al.* 2011). The laser power was 0.3 mW, avoiding laser induced heating of samples. A 50 × objective lens was used giving a laser 'footprint' of 1–3 μm in diameter, with an extended spectral range of 100–2000 $cm^{-1}$. 10 s exposure time and 1 accumulation were acquired for each spectrum, giving a good signal-to-noise ratio. To include the stretching modes of water molecules, extended wavelength (100–4000 $cm^{-1}$) was also measured using the above settings. Spectra were processed using a smooth, baseline subtraction and peak fit functions using WiRE 2.0 software. Peak fitting used a mixture of Gaussian and Lorentzian algorithms.

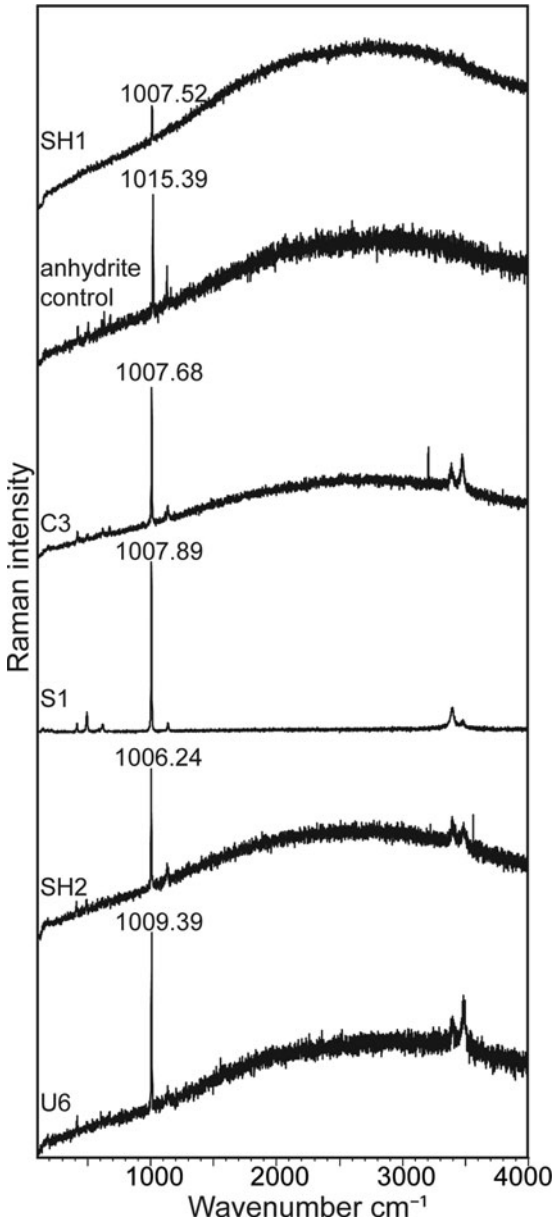


**Fig. 5.** Extended Raman spectra for gypsum and anhydrite (100–4000 $cm^{-1}$). Spectra include v1 sulphate stretching mode and $H_2O$ molecule stretching mode around 3500 $cm^{-1}$.

### *X-ray diffraction*

Diffraction patterns were acquired on powder samples by using an X'Pert diffractometer (PANalytical, NL) equipped with Cu-kα radiation (1.54 Å; 45 kV/40 mA) in θ–θ reflectance geometry; data were collected from 5° to 80° 2θ with a step size of 0.013° and a time-per-step of 13.77 s. Crystalline phases were identified by comparison with ICDD PDF # [01-074-1433] (Gypsum). Samples were powdered by hand using a pestle and mortar.

### *Spectral parameter analysis*

Ten spectra were obtained from each sample and average FWHM were plotted against sulphate band positions.

https://doi.org/10.1017/S1473550416000367 Published online by Cambridge University Press

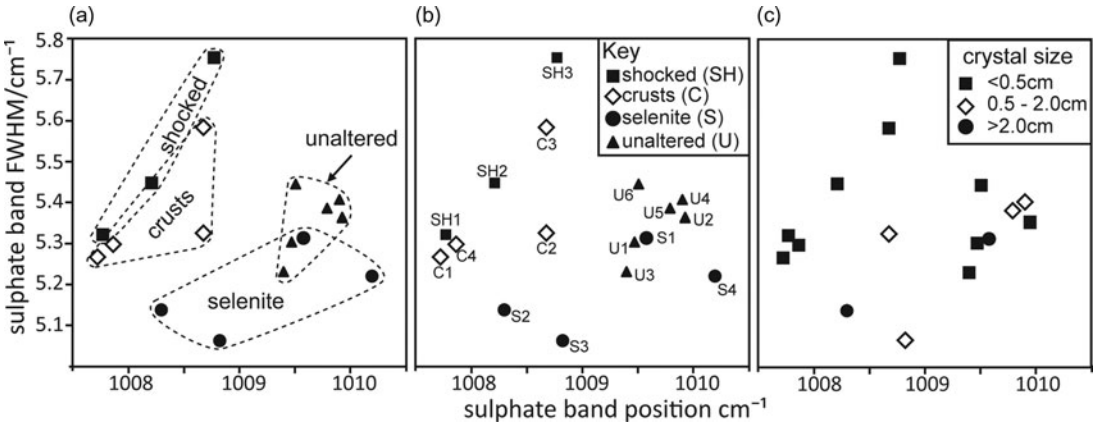


**Fig. 6.** Sulphate band position against sulphate band full width at half maximum (FWHM), with each point representing an average of ten spectra. *x*-axis, is the sulphate (v1) band position in reciprocal centimetres ($cm^{-1}$). *y*-axis, is the sulphate (v1) FWHM. (a) Samples are separated into their geological groups. (b) Samples are distinguished by sample classification (Table 1). (c) Samples are distinguished based on crystal size. Squares denote a crystal size <0.5 cm; diamonds denote a crystal size between 0.5 and 2 cm; circles denote a crystal size >2 cm.

Statistical variance tests were used to determine if sample groups are statistically different from each another.

*Statistical analysis*

Overlapping sample fields were examined using SigmaPlot statistical software package to confirm if the groups were statistically different. The sample groups failed the normality test therefore a non-parametric test was used. As two independent groups were compared, a Man–Whitney U test was used.

## Results

*Raman spectroscopy*

The spectra obtained across the sample set all show a v1 sulphate band position of around 1008 $cm^{-1}$, which is indicative of gypsum (Krishnamurthy & Soots 1971), shown in Fig. 3. The shocked samples, SH2 and SH3, show a sloping baseline with increased signal-to-noise ratio compared with other samples e.g. selenite. Additionally the shocked samples show a weaker Raman signal, with lower band intensities. The spectra from evaporitic crusts are similar spectra to that of shocked samples, with low intensity bands and a higher signal-to-noise ratio, a part from the central uplift crust, which has an improved signal-to-noise ratio. The selenite group, have the cleanest spectra with intense v1 sulphate bands and a better signal-to-noise ratio relative to the shocked samples. Unaltered samples show similar spectra to selenite, except from U6 and U5, which have increased signal-to-noise ratios. Average v1 band positions for each are; unaltered (U) – 1009.615, selenite (S) – 1009.261, shocked (SH) – 1008.251, crusts (C) – 1008.262 $cm^{-1}$. Based on these band positions all samples are classed as gypsum and have not experienced dehydration.

*X-ray diffraction*

Eight gypsum samples were selected from the larger sample set for XRD analysis (Fig. 4), which cover the 4 Ca-sulphate groups. The cell parameters for each sample show that all eight samples are in the form of gypsum. It is common for impact shocked sample to experience partial or complete dehydration, however basanite or anhydrite phases are not found in specimen SH3, which is consistent with the Raman measurements obtained.

## Discussion

*Raman spectroscopy – extended spectra*

Selected samples were re-analysed using an extended wavelength range (100–4000 $cm^{-1}$), to include the stretching modes of water molecules, shown in Fig. 5. An anhydrite control is included to show a completely dehydrated phase. As expected the anhydrite control shows a v1 sulphate band position of 1015.39 $cm^{-1}$, and does not show the stretching modes of water molecules around 3450 $cm^{-1}$. Sample SH1 has a fragment of gypsum, and the spectrum shows a v1 band position of 1007.52 $cm^{-1}$, which is indicative of gypsum, although it does not show the presence of water molecules at the expected wavelength. As shocking promotes devolatilization, the loss of $H_2O$ molecules would be expected, and is well documented by other authors. Additionally, a change in v1 band position from 1008 to 1015 $cm^{-1}$, would also be expected. Sample SH2 shows a band position of 1006.24 $cm^{-1}$, and has the stretching modes of water molecules. This is indicative of gypsum, and suggests that either no dehydration has occurred, or that the specimens have been rehydrated.

Experimental work by Ramkissoon *et al.* (2014) and Bucio *et al.* (2015), clearly show that shocking by impact generates, semi-hydrated and completely hydrated Ca-sulphate phases in the form of basanite and anhydrite, respectively. This can be seen in the v1 sulphate band positon and the presence, or absence, of the stretching modes of water molecules. This relationship does not appear to be realized in naturally impact shocked Ca-sulphates from Haughton crater.

*v1 band position against band FWHM*

The sulphate band position was plotted against the FWHM to determine if these Raman parameters could distinguish

https://doi.org/10.1017/S1473550416000367 Published online by Cambridge University Press

between the gypsum specimens. Fig. 6(a) shows the four types of gypsum used in this study presented as fields. Each point is an average of ten spectra. Selenite has the largest field, which overlaps with unaltered samples. Selenite and unaltered fields plot independently from shocked or crust fields, showing that Raman spectroscopy can distinguish between certain phases of gypsum. The shocked field plots on the edge of the crusts field. Samples with overlapping fields were analysed for statistical significance. No significant difference was found between the shocked and crust sample band positions ($P = 0.966$, Mann–Whitney Sum test) and FWHM ($P = 0.251$), indicating that Raman spectroscopy cannot currently distinguish between impact shocked gypsum and gypsum, which has been dissolved and re-precipitated as a mineral crust. In contrast, a significant difference is evident between selenite and unaltered sample band positions ($P = 0.045$) and FWHM ($P = 0.020$). This shows that using the sulphate v1 band position versus FWHM, differences between gypsum phases are evident. Raman can therefore identify gypsum phases with enhanced habitability.

Figure 6(b) distinguishes samples according to their classification in Table 1. Figure 6(c) distinguishes samples according to crystal size, which was determined petrographically. However, there does not appear to be any control based on crystal size.

## Conclusions

A range of gypsum samples were analysed using Raman spectroscopy, to determine if this technique can differentiate between Ca-sulphates, which have enhanced habitability, and those that do not. Results show that Raman spectroscopy cannot currently determine a significant difference between gypsum, which has been shocked by meteoric impact (enhancing the habitability), and gypsum, which has been dissolved and re-precipitated as an evaporitic crust. Raman spectroscopy is able to differentiate between unaltered gypsum and selenite by plotting v1 sulphate band position against v1 sulphate band FWHM, and as selenite has been found with viable extant microbial colonies at Haughton impact crater, it is regarded as having enhanced habitability.

The presence of $H_2O$ bands in spectra obtained from shocked samples highlights the complexity of Raman spectra observed from naturally shocked samples compared with experimental shock studies. This indicates current capabilities of Raman spectroscopy, for the interpretation of gypsum habitability, prior to its use on the European Space Agency's ExoMars 2020 mission.

## Acknowledgements

This work was funded by STFC grant ST/L001233/1. The University of Aberdeen Raman facility was funded by the BBSRC grant BBC5125101. Thanks to Jo Duncan for XRD assistance.

## References

Beegle, L. *et al.* (2015). SHERLOC : Scanning Habitable Environments with Raman & Luminescence for Organics & Chemicals. In *Aerospace Conference*, 1–8.

Berenblut, B.J., Dawson, P. & Wilkinson, G.R. (1970). The Raman spectrum of gypsum. *Spectrochimica Acta* **27A**, 1849–1863.

Bucio, L. *et al.* (2015). Phase transitions induced by shock compression on a gypsum mineral: X-ray and micro-Raman analysis. *High Press. Res.* **35**(4), 355–362.

Cabrol, N.A. *et al.* (1999). Hydrogeologic evolution of Gale Crater and its relevance to the exobiological exploration of Mars. *Icarus* **139**, 235–245.

Chapman, C.R. & Jones, K.L. (1977). Cratering and obliteration history of Mars. *Annu. Rev. Earth Planet. Sci.* **5**, 515–540.

Cockell, C.S. *et al.* (2002). Impact-induced microbial endolithic habitats. *Meteorit. Planet. Sci.* **37**, 1287–1298.

Cockell, C.S. *et al.* (2003). Measurements of microbial protection from ultraviolet radiation in polar terrestrial microhabitats. *Polar Biol.* **26**, 62–69.

Ellery, A. & Wynn-Williams, D. (2003). Why Raman spectroscopy on Mars ?—a case of the right tool for the right job. *Astrobiology* **3**(3), 565–579.

Farmer, J.D. & Des Marais, D.J. (1999). Exploring for a record of ancient Martian life. *J. Geophys. Res.* **104**, 26,977–26,995.

Haskin, L.A. *et al.* (1997). Raman spectroscopy for mineral identification and quantification for *in situ* planetary surface analysis : a point count method. *J. Geophys. Res.* **102**(97), 19293–19306.

Hogan, J.D. *et al.* (2012). Micro-scale deformation of gypsum during micro-indentation loading. *Int. J. Rock Mech. Mining Sci.* **54**, 140–149.

Jehlička, J., Edwards, H.G.M. & Oren, A. (2014). Raman spectroscopy of microbial pigments. *Appl. Environ. Microbiol.* **80**(11), 3286–3295.

Krishnamurthy, N. & Soots, V. (1971). Raman spectrum of gypsum. *Can. J. Phys.* **49**, 885–896.

Lane, N. & Martin, W.F. (2012). The origin of membrane bioenergetics. *Cell* **151**(7), 1406–1416.

Lindgren, P. *et al.* (2009). Preservation of biological markers in clasts within impact melt breccias from the Haughton impact structure, Devon Island. *Astrobiology* **9**(4), 391–400.

Liu, Y., Wang, A. & Freeman, J.J. (2009). Raman, MIR, and NIR spectroscopic study of calcium sulphates: Gypsum, bassanite, and anhydrite. In *40th Lunar and Planetary Science Conference*. p. 2128.

Naumov, M.V. (2002). Impact-generated hydrothermal systems: Data from Popigai, Kara, and Puchezh-Katunki impact structures. In: Plado, J. and Pesonen, L.J. (Eds.), *Impacts in Precambrian shields*. Springer-Verlag, Berlin, pp. 117–171.

Newsom, H.E., Hagerty, J.J. & Thorsos, I.E. (2001). Location and sampling of aqueous and hydrothermal deposits in Martian impact craters. *Astrobiology* **1**(1), 71–88.

Osinski, G.R. & Spray, J.G. (2001). Impact-generated carbonate melts: evidence from the Haughton structure, Canada. *Earth Planet. Sci. Lett.* **194**(1–2), 17–29.

Osinski, G.R., Spray, J.G. & Lee, P. (2005). A case study of impact-induced hydrothermal activity: the Haughton impact structure, Devon Island, Canadian High Arctic. *Meteorit. Planet. Sci.* **40**(12), 1789–1812.

Parnell, J. *et al.* (2004). Microbial colonization in impact-generated hydrothermal sulphate deposits, Haughton impact structure, and implications for sulphates on Mars. *Int. J. Astrobiol.* **3**(3), 247–256.

Pérez, F.R. & Martinez-Frias, J. (2006). Raman spectroscopy goes to Mars. *Spectrosc. Eur.* **18**(1), 18–21.

Prasad, P.S.R., Pradhan, A. & Gowd, T.N. (2001). *In situ* micro-Raman investigation of dehydration mechanism in natural gypsum. *Curr. Sci.* **80** (9), 1203–1207.

Ramkissoon, N.K. *et al.* (2014). Examining impact induced mineral devolatilisation using Raman spectroscopy. In *45th Lunar and Planetary Science Conference*. p. Abstract 1891.

Robertson, P.B. & Sweeney, J.F. (1983). Haughton impact structure: structural and morphological aspects. *Can. J. Earth Sci.* **20**(7), 1134–1151.

https://doi.org/10.1017/S1473550416000367 Published online by Cambridge University Press

Rossi, A.P. *et al*. (2008). Large-scale spring deposits on Mars? *J. Geophys. Res. E: Planets* **113**(8), 1–17.

Rull, F. *et al*. (2011). The Raman Laser Spectrometer (RLS) on the ExoMars 2018 Rover Mission. In *42nd Lunar and Planetary Science Conference*.

Schwenzer, S.P. *et al*. (2012). Gale crater: formation and post-impact hydrous environments. *Planet. Space Sci*. **70**(1), 84–95.

Sherlock, S.C. *et al*. (2005). Re-evaluating the age of the Haughton impact event. *Meteorit. Planet. Sci*. **40**(12), 1777–1787.

Thomson, B.J. *et al*. (2011). Constraints on the origin and evolution of the layered mound in Gale Crater, Mars using Mars Reconnaissance Orbiter data. *Icarus* **214**(2), 413–432.

Wang, A., Haskin, L.A. & Cortez, E. (1998). Prototype Raman spectroscopic sensor for *in situ* mineral characterization on planetary surfaces. *Appl. Spectrosc*. **52**(4), 477–487.

Wray, J.J. *et al*. (2010). Identification of the Ca-sulfate bassanite in Mawrth Vallis, Mars. *Icarus* **209**(2), 416–421.

https://doi.org/10.1017/S1473550416000367 Published online by Cambridge University Press